

Classification of In-vivo Endomicroscopic Images of the Alveolar Respiratory System

Caroline Petitjean, Jonathan Benoist
 Université de Rouen, LITIS EA 4108
 BP 12, 76801 Saint-Etienne-du-Rouvray, France
 Caroline.Petitjean@univ-rouen.fr,
 Jonathan.Benoist@free.fr

Luc Thiberville, Mathieu Salaün
 CHU de Rouen, LITIS EA 4108
 1 rue de Germont, 76000 Rouen, France
 Luc.Thiberville@univ-rouen.fr,
 Mathieu.Salaün@univ-rouen.fr

Laurent Heutte
 Université de Rouen, LITIS EA 4108
 BP 12, 76801 Saint-Etienne-du-Rouvray, France
 Laurent.Heutte@univ-rouen.fr

Abstract

This paper presents an original system for the automatic classification of normal versus abnormal endomicroscopic images of the respiratory alveolar system. Images from the alveoli were acquired in-vivo using a newly developed technique, based on confocal microscopy. The classification process includes a 120-feature extraction step followed by an SVM based classification. Results are excellent for non-smoker images and demonstrate the great help of this system for computer-aided diagnosis, using confocal microscopy.

1 Introduction

1.1 Medical background

The lungs are the essential respiration organ. They are divided into two anatomic and functional regions:

- the air conduction system, that includes the trachea, bronchi, and bronchioles,
- and the gas-exchange region, or lung parenchyma, made of alveolar sacs. These sacs are made up of clusters of alveoli, tightly wrapped in blood vessels, that allow for gas exchange.

Whereas the conduction airways can be explored in vivo during bronchoscopy, the alveolar region was until recently unreachable for in vivo morphological investigation. Therefore, the pathology of the distal lung is currently assessed only in vitro, using invasive techniques such as open lung biopsies. No real time imaging was available.

A new endoscopic technique, called Fibered Confocal Fluorescence Microscopy (FCFM), has recently been developed that enables the visualisation of the more distal regions of the lungs in-vivo [8]. The technique is based on the principle of fluorescence confocal microscopy, where the microscope objective is replaced by a fiberoptic miniprobe, made of thousands of fiber cores. The miniprobe can be introduced into the 2mm working channel of a flexible bronchoscope to produce in-vivo endomicroscopic imaging of the human respiratory tract in real-time. Real-time

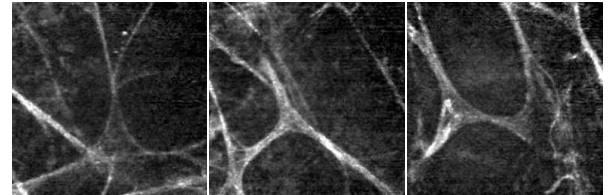


Figure 1: FCFM images of healthy cases

alveolar images are continuously recorded during the procedure and stored for further analysis. This very promising technique could replace lung biopsy in the future and might prove to be helpful in a large variety of diseases, including interstitial lung diseases [9].

A clinical trial is currently being conducted that collects FCFM images in several pathological conditions of the distal lungs. This trial also includes a control group of smoker and non smoker healthy volunteers. This strategy provides a dataset of normal images, that can be compared with pathologic ones.

The images recorded within the alveolar regions of the lungs have not been very well described so far. These images represent the alveolar structure, made of elastin fiber (Figure 1), with an approximate resolution of $1\mu\text{m}$ per pixel. This structure appears as a network of (almost) continuous lines. This elastic fiber framework can be altered by distal lung pathologies and as one can see on Figure 2, images acquired on pathological subjects differ from the ones acquired on healthy subjects. The great complexity of these new images justifies the development of reproducible software tools for computer aided diagnosis, that enables automatic image description for diagnosis and follow up of pathological situations.

1.2 Aim of the study

The aim of the study is to conceive and develop methods for automatic analysis of FCFM images, so as to discriminate healthy cases from pathological cases. In order to perform this 2-class classification, the system relies on 60 annotated images acquired

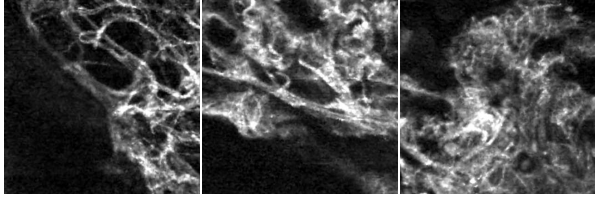


Figure 2: FCFM images of pathological cases

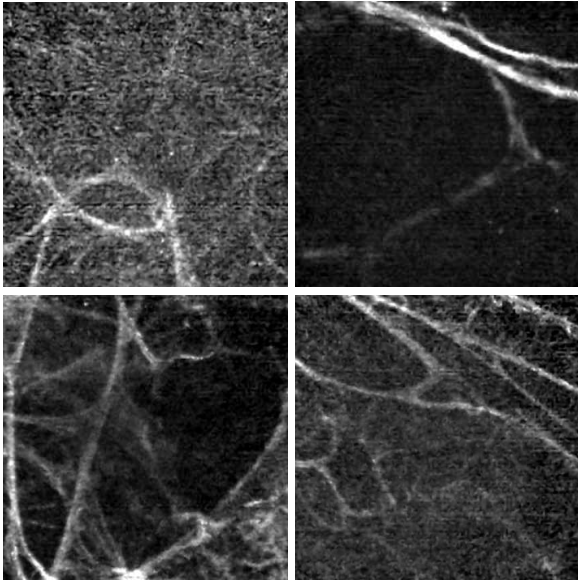


Figure 3: Difficult cases in FCFM images: healthy subjects (top), pathological subjects (bottom)

during the clinical trial, coming from both healthy (38) and pathological (22) cases.

The remaining of this paper is organized as follows: our classification method is described in Section 2, and results and discussion are provided in Section 3. Section 4 concludes and draws some perspectives for this work.

2 Image classification method

As usual in data classification methods, our system includes a feature extraction step and a classification step [4].

2.1 Feature extraction

Features must be chosen to allow the discrimination between healthy and pathological subjects. As shown in Figure 3, some images present difficulties where pathological cases can be visually misclassified for healthy ones and vice versa. The choice of features is therefore critical.

Several general characteristics can be observed from the visual analysis of the images. As shown in Figure 1, the alveolar structure in healthy subjects can be described as contrasted continuous lines and curves. On the opposite, in the pathological subset, the disorganization of the meshing is illustrated by the numerous irregularities and the tangle of the

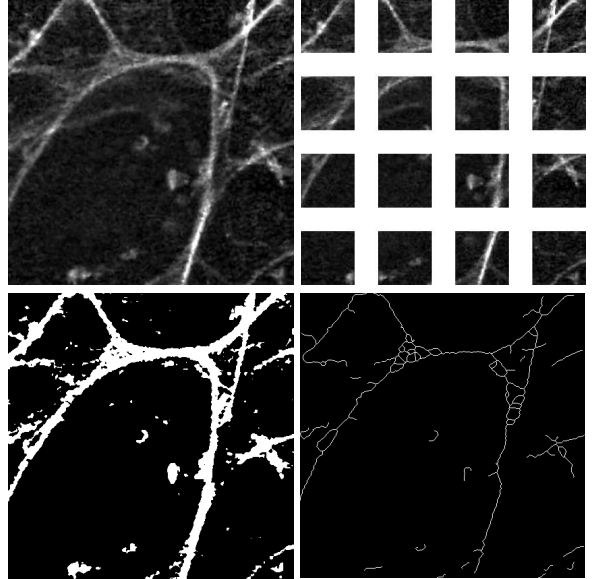


Figure 4: From left to right, top to bottom: original FCFM image, 16 subwindows, binarized image, skeleton on binarized image

fibered structures (see Figure 2). Differences are mostly visible for the structure shape, image texture and contrast implying that numerical features must therefore be chosen among the ones that best describe the visual differences from these three points of view.

The **structure contrast** can be characterized by studying first order pixel gray level distribution and computing pixel densities. Because structures also show local differences, local parameters are computed on subwindows of the image. Subwindows are obtained by dividing by 4 the image height and width (Figure 4). Features characterizing the image contrast are:

- first order statistics on global and local histogram: mean, variance, skewness, kurtosis, entropy ;
- global and local pixel densities obtained on binarized images using Otsu thresholding;
- the sum of the image gradient values, obtained using Prewitt operator.

We could suppose that pathological images will have high values for densities, since a large number of pixels having high value cover a large part of the image.

The **complexity of the structure shape** can be characterized by studying the image skeleton. After skeletonization [3] obtained on the binary image, the number of junction points is computed. One can suppose that on clearly organized, healthy images, this number will be small, contrary to pathological images where the meshing mess will induce a higher number of points.

The **image texture** can be characterized by Haralick parameters computed from cooccurrence matrix [6]: energy, contrast, homogeneity, correlation, along 4 directions (0° , 45° , 90° , 135°).

A total of 120 features are computed, as shown in Table 1.

Table 1: Features used to characterize FCFM images

	Features	Number
Contrast	Global histogram statistics	5
	Local histogram statistics	80
	Density	1
	Local densities	16
	Sum of image gradient	1
Shape	Number of junction points in skeleton	1
Texture	Haralick parameters	16
	Total	120

2.2 Classifier

On the previously cited features a Support Vector Machine (SVM) classifier is implemented [10]. SVM is one of the most performing and most used classification algorithm. The support vector machine classifier is a binary classifier algorithm that looks for an optimal hyperplane as a decision function in a high-dimensional space. A classical choice for the kernel is the polynomial kernel.

In order to improve the prediction performance of the classifier, and to provide faster and more cost-effective decision, variable selection [5] can be used. It can also provide a better understanding of which visual features discriminate the data. Support Vector Machine - Recursive Feature Elimination (SVM-RFE) is one way to perform variable selection [7]. The goal is to find a subset of size r among d variables ($r < d$) which maximizes the performance of the predictor. The method is based on a sequential backward selection. One feature at a time is removed until r features are left. The removed variables are the ones that minimize the variation of the margin.

2.3 Learning and test base constitution

FCFM images are now to be divided into a learning base and a test base. Because of the small number of images, a cross validation process is used, which consists in dividing the image base into n folds ($n = 3$ here). Two folds are used for learning and the last one for testing. Performance are averaged on the three folds. Cross validation is also randomly sampled 500 times, so as to make accuracy more reliable and reduce the bias. Performance given in Section 3 are then averaged on these 500 trials and variance is also computed.

Because of the large difference between non-smoker and smoker images, experiments have been conducted separately on those two groups (Table 2). Indeed, alveolar fluorescence imaging in smokers dramatically differs from imaging in non-smokers. Whereas FCFM exclusively images the elastin framework of the alveolar ducts in non-smokers, in smokers, tobacco-tar induced fluorescence allows to observe the alveolar walls and the presence of macrophages (cells which digest cellular debris), as shown in Figure 5.

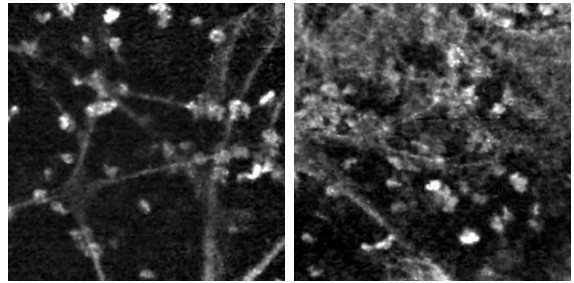


Figure 5: FCFM images of smoker, healthy (left) and pathological (right) cases. Notice the presence of macrophages.

Table 2: Number of images

	Healthy subjects	Pathological subjects
Non smoker	23	10
Smoker	15	12
Total	38	22

3 Results

The SVM classifier and SVM-RFE based feature selection [7] are implemented using the SVM and Kernel Methods Matlab Toolbox [2]. The system performance is assessed with correct classification rate for both classes, false negative rate, which is the proportion of healthy instances that were erroneously reported as pathological and false positive rate, which is the proportion of pathological cases considered healthy. Variance is computed over the cross validation sampling. Other statistical measures used to assess the performance of our system are recall, which is the number of healthy cases recognized as healthy, divided by the total number of healthy cases in the database, and precision, which measures the number of healthy cases recognized as healthy, divided by the total number of cases recognized as healthy by the system.

Results on non-smoker images. These results, shown in Table 3, are excellent for the considered database. Thanks to feature selection, the number of features, initially 120, drops down to 33, without modification in the performance. The selection of relevant variables allows to gain some insight about the usefulness of features: the most discriminating ones are texture-based features, the local pixel densities and the sum of image gradient, which highlights the importance of local, contrast-based differences between healthy and pathological subjects.

Results on smoker images. Results are less satisfying as shown in Table 4. Chosen features do not seem to be adequate for discriminating healthy and pathological subjects. They could be improved by the use of other features such as for example Haar wavelets, Gabor filters, or by drastically increasing the number of features. Other classifiers, such as random forests for instance, could also help to make classification more reliable [1]. Note also that feature selection reduces the number of features only to 98, not showing a real inter-

Table 3: Results on the non-smoker image base

Feature number	Without/with feature selection
	120 / 33
Classification rate	1.00
Error rate	0.00
Variance	0.00
False positive	0.00
False negative	0.00
Recall	1.00
Precision	1.00

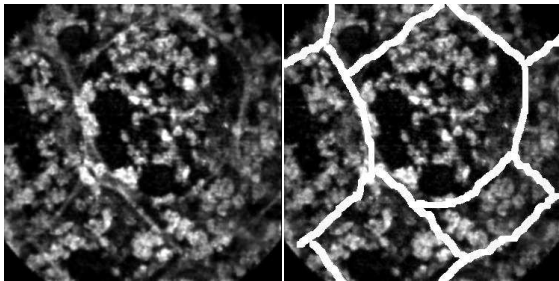


Figure 6: FCFM images of smoker, showing how the line network is hidden behind the macrophages. Network is highlighted on the right image.

est in variable selection, despite a slight increase of the classification rate. Retained features are texture-based features, local pixel densities, the sum of image gradient and local histogram statistics. Global contrast features and the number of junction points seem to be of no interest, because the line network is hidden behind macrophages, making it difficult to characterize the structure (Figure 6).

Table 4: Results on the smoker image base

	Without feature selection	With feature selection
Feature number	120	98
Classification rate	0.80	0.83
Error rate	0.20	0.17
Variance	0.10	0.09
False positive	0.23	0.16
False negative	0.17	0.18
Recall	0.83	0.82
Precision	0.82	0.87

4 Conclusions

The present work deals with the classification of a new category of images from the distal lung. The images were acquired using a fibered confocal fluorescence microscopy, a technique that enables the observation of in vivo alveolar structures for the first time. Such images are not well described so far, and difficult to discriminate by pathologists and respiratory physicians. Our classification system, that aims at discriminating healthy cases from pathological ones, shows excellent performance for non smoker images. However, the corresponding database should be extended to confirm these results, by extending the

image dataset. Because the clinical trial is ongoing, this will be feasible in the near future. Conversely, the classification rate on smoker images is lower (83%), and needs to be improved by using other texture-oriented features, as well as more reliable classifiers such as random forests for example.

Future work will also concern rendering the process real-time, so as to aid the clinician during examination in real time. Classification methods could also give information about which part of the image is the most discriminant or which part of the structure might be more altered by pathologies. A future goal will also be to discriminate between different pathologies : interstitial lung diseases (abestosis, systemic sclerosis, fibrosis, sarcoidosis), carcinomatous lesions etc.

References

- [1] L. Breiman: "Random forests", *Machine Learning*, vol.45, p.5-32, 2001.
- [2] S. Canu, Y. Grandvalet, V. Guigue and A. Rakotomamonjy: "SVM and Kernel Methods Matlab Toolbox", *Perception Systèmes et Information, INSA de Rouen, Rouen, France*, 2005.
- [3] G.S. Dibajaa and E. Thiel: "Skeletonization algorithm running on path-based distance maps", *Image and Vision Computing*, vol.14, p.47-57, 1996.
- [4] R.O. Duda and P.E. Hart: "Pattern Classification and Scene Analysis," *John Wiley & Sons*, 1973.
- [5] I. Guyon and A. Elisseeff: "An introduction to variable and feature selection", *Journal of Machine Learning Research*, vol.3, p.1157-1182, 2003.
- [6] R.M. Haralick, K. Shanmugam and I. Dinstein: "Textural Features for Image Classification," *Systems, Man and Cybernetics*, vol.3, no.6, p.610-621, 1973.
- [7] A. Rakotomamonjy: "Variable selection using SVM-based criteria," *Journal of Machine Learning Research*, 3:1357-1370, 2003.
- [8] L. Thiberville, S. Moreno-Swirc, T. Vercauteren, E. Peltier, C. Cave and G. Bourg-Heckly: "In vivo imaging of the bronchial wall microstructure using fibered confocal uorescence microscopy," *American Journal of Respiratory and Critical Care Medicine*, vol.175, no.1, p.22-31, 2007.
- [9] L. Thiberville, G. Bourg-Heckly, M. Salaün, S. Dominique and S. Moreno-Swirc: "Human in-vivo confocal microscopic imaging of the distal bronchioles and alveoli," *Chest Journal*, vol.132, no.4, p.426, 2007.
- [10] V. Vapnik: "The nature of statistical learning theory," *Springer*, 1995.